

# Corrosion Analysis of Friction Stir-Welded Brass-Brass and Copper-Copper Plates

Ajay Kumar V<sup>\*1</sup>, K Pavani<sup>2</sup> and K Mahesh<sup>3</sup>

<sup>1,3</sup>*Department of Metallurgical and Materials Engineering*

<sup>2</sup>*Department of Chemistry*

*Rajiv Gandhi University of Knowledge Technologies, Basar, Adilabad, Telangana, India 504107.*

[ajay@rgukt.ac.in](mailto:ajay@rgukt.ac.in)

## Abstract

Friction stir-welding has become widely practiced in the fabrication of light-weight structures requiring high strength-to-weight ratios and superior corrosion resistance. The friction stir-welding (FSW) process and tool parameters play a key role in determining the joint's characteristics. In this paper, Copper-copper and brass-brass plates were welded using friction stir welding machine at same rotational and transverse speeds. The corrosion resistance behavior of friction stir-welded copper-copper and brass-brass joints along with parent copper and brass plates were studied via polarization and weight loss method. The microstructures were examined to observe corrosion resistance. Energy Dispersive Spectroscopy was conducted to know elemental composition of parent metals. Optical microscope was used to obtain the microstructures of parent, welded and corroded plates. The experimental results indicated that the welding process has a major effect on the corrosion resistance, as the weld joint acts as a cathode and gives better resistance to corrosion when compared to parent plates.

Key words: Friction stir welding, corrosion, polarization, Hardness, microstructure.

## Introduction

Friction stir welding is one of the solid state welding processes which has gained enormous interest in present day research as it involves a welding process produced by softening, plastic deformation combined with forging action caused by tool rotation of base metal [1–4]. Absence of melting of base metal in FSW reduces oxidation, residual stress, solidification related defects. In recent times many reports on friction stir welding of various metal system such as aluminium [5–9], magnesium [10, 11], mild steel [12], stainless steel [13] have been published.

Welding of copper is usually difficult by conventional fusion techniques due to the deteriorative influence of oxygen, impurities and also because of its high thermal diffusivity

which is about 10–100 times higher than that of steels. In other words, the greater dissipation of heat through copper work-piece requires higher heat input for welding in comparison with other materials, resulting in quite low welding speeds. During arc welding of copper and copper alloys, oxygen segregates on grain boundaries of metal. This can lead to embrittlement of the weld joint. Precipitation hardenable copper alloys may lose their alloying elements (Zn) through oxidation during fusion welding, compromising their strength. Copper welds frequently suffer from lack of fusion because of the high thermal conductivity of copper as it reduces the concentration of heat needed to melt a critical mass of metal and ensures complete filling of the weld cavity. Preliminary studies on the FSW for copper to copper [14–16] and brass [17–20] have also been reported earlier.

In view of huge commercial importance of copper alloys and required for joining in fabrication of engineering components, this work was an attempt to study the corrosion resistance of friction stir welded copper–copper and brass–brass plates. The microstructure of the weld joints were observed before and after corrosion using optical microscope and mechanical properties such as hardness were determined. This work would help in understanding structure property relationship to construct and fabricate new components.

## Experimental Procedure

Copper and Brass alloy plates (length×breadth×thickness=60×40×6mm) were used in this present work. The chemical compositions of parent species were obtained from energy dispersive X-ray spectroscopy attached to FESEM (EDX INCA, OXFORD Instruments.) and measurements are presented in Table 1 and Table 2. The joints were fabricated by friction stir welding machine Biss-ITS. The tool bit used in this experiment made up of hot die steel– H13, designed as shown in figure 1 and has the hardness of 35.5 HRC. The welding parameters used are shown in Table 3. Microstructure evaluation is carried out using Optical microscope (Leica Microsystems DMI5000M) and the images were taken in the magnification range of 20X–50X. For corrosion study potentiodynamic polarization test was conducted as per the standard ASTM G 59–97 using potentiostat (IEC 61326, IVIUM technologies, Netherland) on friction stir welded copper–copper and brass–brass weld joints. The two welded plates (Copper–Copper & Brass–Brass) interface junction was compared with the parent metal. In this study a corrosive environment 0.2N HCl was used. Along with this, detailed corrosion study was carried out by immersion method (in 0.2N HCl) as well as salt spray (in 5% NaCl) methods. The parent and welded plates were polished by different grades of emery sheets to remove impurities present on the surface. The plates after corrosion were used as such to study the microstructure which is then compared with parent and welded plates respectively.

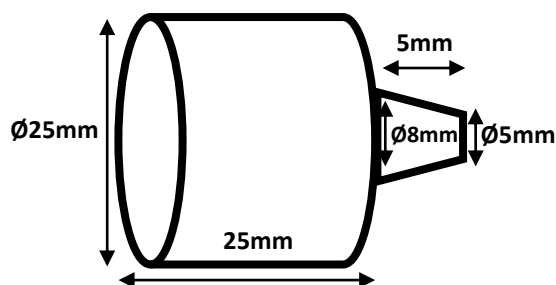


Figure 1. Tool bit dimension used in friction stir welding

Table:-1 Chemical composition of copper sample

Element	Cu	Si	Al	O <sub>2</sub>	C
Wt%	126.83	0.55	0.61	1.35	8.67

Table:-2 Chemical composition of brass

Element	Cu	Zn	Fe	Al	O <sub>2</sub>	C
Wt%	80.54	58.31	0.87	0.47	2.05	12.61

Table:-3 Parameters taken for friction welding

Parameters	Speed of rotation (rpm)	Feed Speed (mm/min)	Burn off length (mm)
	950	80	30

## Corrosion study

### Potentiodynamic polarization curves (PR)

A typical three-electrode electrochemical corrosion cell was used in all the experiments. A saturated calomel electrode (SCE) was used as reference. All measured potentials were referred to this electrode. A platinum foil was used as the counter electrode. Then four plates parent copper, parent brass, Friction stir welded copper-copper and friction stir welded brass-brass plates were used as working electrodes. All experiments were carried out using ordinario without supporting neither electrolyte nor deareation. A potentiostat, controlled by a personal computer, equipped with a GPIB card and the commercial software was employed to obtain the potentiodynamic polarization curves. Before each experiment, the open circuit potential (OCP) was recorded for at least 30 min. Polarization curves was obtained potentiodynamically; the linear potential sweep was performed at a  $\pm 248$  mV potential window around the measured OCP, from the cathodic to the anodic side, at scan rates of 0.1 and 1 mV s<sup>-1</sup>.

## Salt Spray method (SS)

Salt spray testing was conducted in accordance with ASTM B117 at Assured Testing Services, Ridgway, PA. This practice provides a controlled corrosive environment that has been utilized to produce relative corrosion resistance information for specimens of metals exposed in a test chamber. Prediction of performance in natural environments has seldom been correlated with salt spray results when used as stand-alone data. The apparatus for salt spray (fog) exposure consists of a fog chamber, a salt solution reservoir, a supply of suitably conditioned compressed air, one or more atomizing nozzles, specimen supports, provision for heating the chamber, and necessary means of control. Drops of the solution that accumulate on the ceiling or cover of the chamber shall not be permitted to fall on the specimens being exposed. Drops of solution that fall from the specimens shall not be returned to the solution reservoir for re-spraying. All the four specimens were tested per material/process condition.

## Immersion method (IM)

Polished specimens were initially weighed in an electronic balance. Weighed plates are immersed in 100 mL of the acid (0.2 N HCl). After 72 hrs, they were taken out and then washed thoroughly with tap water, rinsed with distilled water, dried, stored in desiccators and reweighed. From the change in weight of specimens the corrosion rate was calculated using the following relationship,

$$\text{Corrosion Rate (mpy)} = \frac{534 \times \Delta W}{(A \times T \times D)}$$

$\Delta W$  = Loss in weight in mg

A = surface area of the specimen (inch<sup>2</sup>)

T = Time in hrs

D = Density in g/cc

Using the above expression corrosion rates were calculated for all four plates and tabulated in Table 6 and Table 9.

## Results and Discussion

### Corrosion study analysis of Brass Plates

#### Potentiodynamic polarization method

Polarization resistance measurements are an accurate and rapid way to measure the general corrosion rate. Electrochemical polarization test methods are extremely pertinent

for understanding and evaluating the corrosion resistance of materials and the effect of changes in the corrosive environment. They can establish criteria for anodic or cathodic protection and susceptibility to several forms of corrosion.

Figure 2 shows the potentiodynamic polarization curves of brass and friction stir welded brass–brass in 0.2N HCl. Kabasakaloglu et al. [21] have concluded that the corrosion process of brass in HCl media starts at  $-1.0$  V vs SCE, with the subsequent formation of  $\text{ZnO}/\text{Zn(OH)}_2$  and zinc ions. According to the authors, dissolution of copper is prevented up to the  $\text{CuCl}$  formation potential. Peaks observed at very negative potentials, i.e., around  $-1.3$  V, have been attributed to the formation of  $\text{ZnO}/\text{Zn(OH)}_2$ . However, this peak at very negative potentials has not been much studied yet.

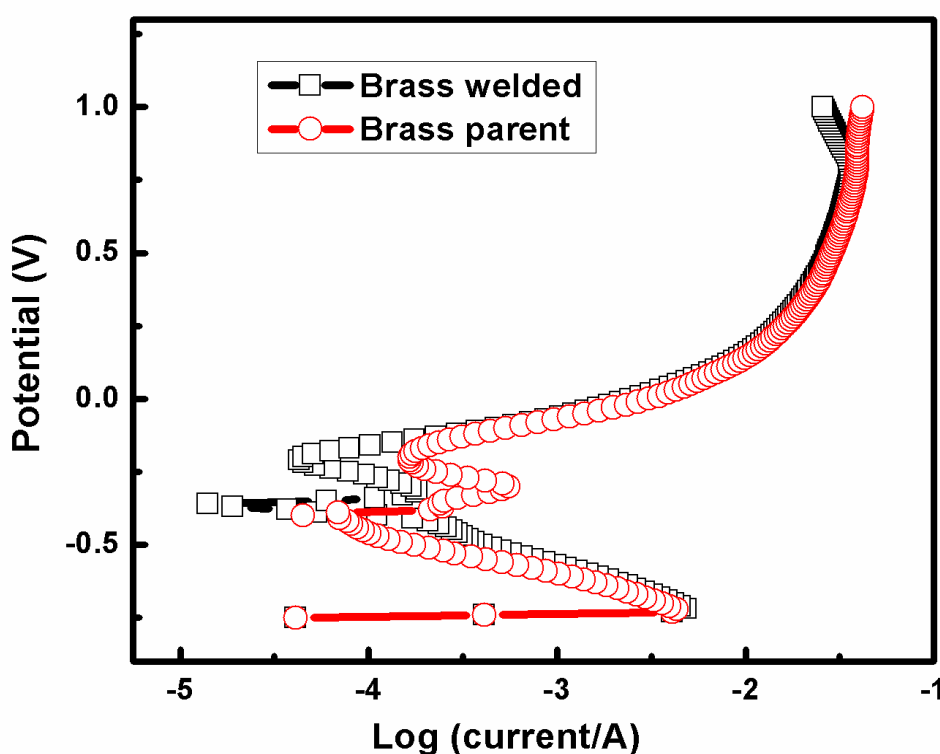
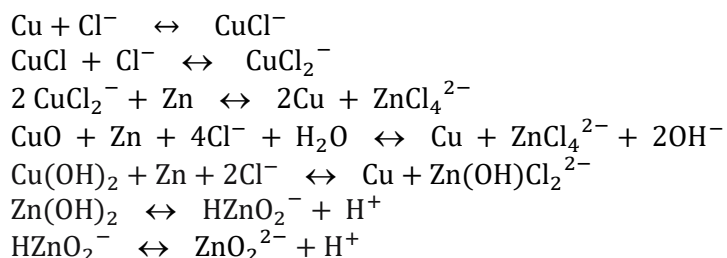


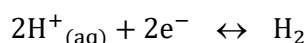
Figure 2. potentiodynamic polarization curves of brass and friction stir welded brass–brass in 0.2N HCl

Morales et al. [22, 23], among others, have demonstrated that the dissolution of zinc takes place with anodic polarization even in the passive region. Actually, they showed that the passive layer formed on Cu–Zn alloys in chloride-buffered media consists of a film whose composition is  $\text{ZnO} \cdot x\text{H}_2\text{O} + \text{Cu}_2\text{O} + \text{CuO}/\text{Cu(OH)}_2 + \text{CuCl}$  [24–26]. During the anodic polarization, the dissolution of the passive film occurs above a certain potential, known as the breakdown potential,  $E_b$ , which shifts negatively as the chloride concentration increases. The authors have also concluded that brass is less resistant to corrosion than copper. The

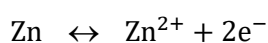
breakdown of the passivity has been attributed to the formation of soluble species, i.e., chloro- and/or oxycomplexes.



In the present paper, a comparative study is performed on the voltammetric behavior of brass and friction stir welded brass–brass specimens. Polarization resistance can be related to the rate of general corrosion for metals at or near their corrosion potential,  $E_{\text{corr}}$ . The figure 2 clarifies typical Tafel behavior that is greatly differing from that obtained for brass. This is because, for the active zinc metal in acid solutions, when dissolved in presence of oxygen, both hydrogen evolution and oxygen reduction reactions will be possible. However, in view of the fact that, the saturated solubility of oxygen in pure water at 25°C is only about  $10^{-3} \text{ mol dm}^{-3}$  [27] and decreases slightly with increasing the concentration of dissolved salts. In addition, the concentration of  $\text{H}_3\text{O}^+$  in acid solutions, at  $\text{pH} \approx 0$ , is high, and since this ion has a high rate of diffusion, consequently, the contribution of the hydrogen evolution reaction at the cathodic process will overcome the oxygen reduction reaction. Therefore, the corrosion of zinc in acid solution proceeds via two partial reactions [28–29]. The partial cathodic reaction involves evolution of hydrogen gas.



The partial anodic reaction involves the oxidation of Zn and formation of soluble  $\text{Zn}^{2+}$



The results of the polarization curve are shown in Table 4 in presence of 0.2N HCl at room temperature. It is observed that the parent brass metal shows high corrosion rate of 0.2549 mm per year while friction stir welded brass imparts 0.1049 mm per year and it has better corrosion resistance. It is also to be noted that the corrosion current is also higher for the parent metal compared to the welded junction. This result indicate that in the friction stir welded brass sample, the weld joint act as a cathode and give better resistance to corrosion when compared to parent brass plates.



Table 4:– Results of the polarization curve of parent brass and friction stir welded brass–brass plates

Sample	$i_{corr}$ (Corrosion current density in mA/cm <sup>2</sup> )	Corrosion rate in mm/year	Corrosion rate in mpy	area of the plates in cm <sup>2</sup>	Polarisation Resistance $R_p$
Brass	7.79E–5	0.2549	10.035	1	423.5
FSW Brass–Brass	3.207E–5	0.1049	4.129	1	443.6

## Salt Spray and Immersion Methods

The results of salt spray method shown in Table 5 and immersion method in Table 6 are completely in agreement with the polarization data showing that the friction stir welded brass plate shows low corrosion rate compared to parent brass plate.

Table 5:– Salt Spray method

Sample	Medium	$\Delta W$ (mg)	CR=534 $\Delta W$ /DAT
Brass plate	5% NaCl	11 mg	27.87mpy
FSW brass–brass	5% NaCl	3.7 mg	9.299 mpy

Table 6:– Immersion Method

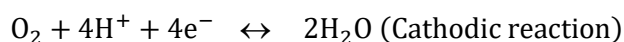
Sample	Medium	$\Delta W$ (mg)	CR=534 $\Delta W$ /DAT
Brass plate	0.2 N HCL	130.1 mg	27.47 mpy
FSW brass–brass	0.2 N HCL	79.4 mg	16.63 mpy

## Corrosion study analysis of Copper Plates

Figure 3 shows the potentiodynamic polarization curves of copper in 0.2N HCl. The electrochemical potentiodynamic polarization parameters, i.e. corrosion potential ( $E_{corr}$ ) and the corrosion current density ( $i_{corr}$ ), obtained from the intersection of the anodic and cathodic Tafel lines with the corresponding corrosion potential are given in Table 7. It has been shown that in the Tafel extrapolation method, use of both the anodic and cathodic Tafel regions is undoubtedly preferred over the use of only one Tafel region [30]. The corrosion rate can also be determined by Tafel extrapolation of either the cathodic or anodic polarization curve alone. If only one polarization curve alone is used, it is generally the cathodic curve which usually produces a longer and better defined Tafel region. Anodic

polarization may sometimes produce concentration effects, due to passivation and dissolution, as well as roughening of the surface which can lead to deviations from Tafel behavior.

The cathodic parts of the polarization curves show limiting current corresponds to the oxygen reduction reaction. This indicates that the cathodic process is controlled by diffusion of oxygen gas from the bulk solution to the metal surface. This behavior is well known since copper can hardly be corroded in the deoxygenated dilute hydrochloric acid [31], as copper cannot displace hydrogen from acid solutions according to theories of chemical thermodynamics. However, in aerated hydrochloric acid, dissolved oxygen is reduced on copper surface and this will enable some corrosion to take place [32]. Cathodic reduction of oxygen can be expressed either by two consecutive  $2e^-$  steps involving a reduction to hydrogen peroxide first followed by a further reduction to water or by a direct  $4e^-$  transfer step as shown by below equation.



The partial anodic reaction involves the oxidation of Cu and formation of soluble  $Cu^{2+}$   
 $Cu \leftrightarrow Cu^{2+} + 2e^-$  (Anodic reaction)

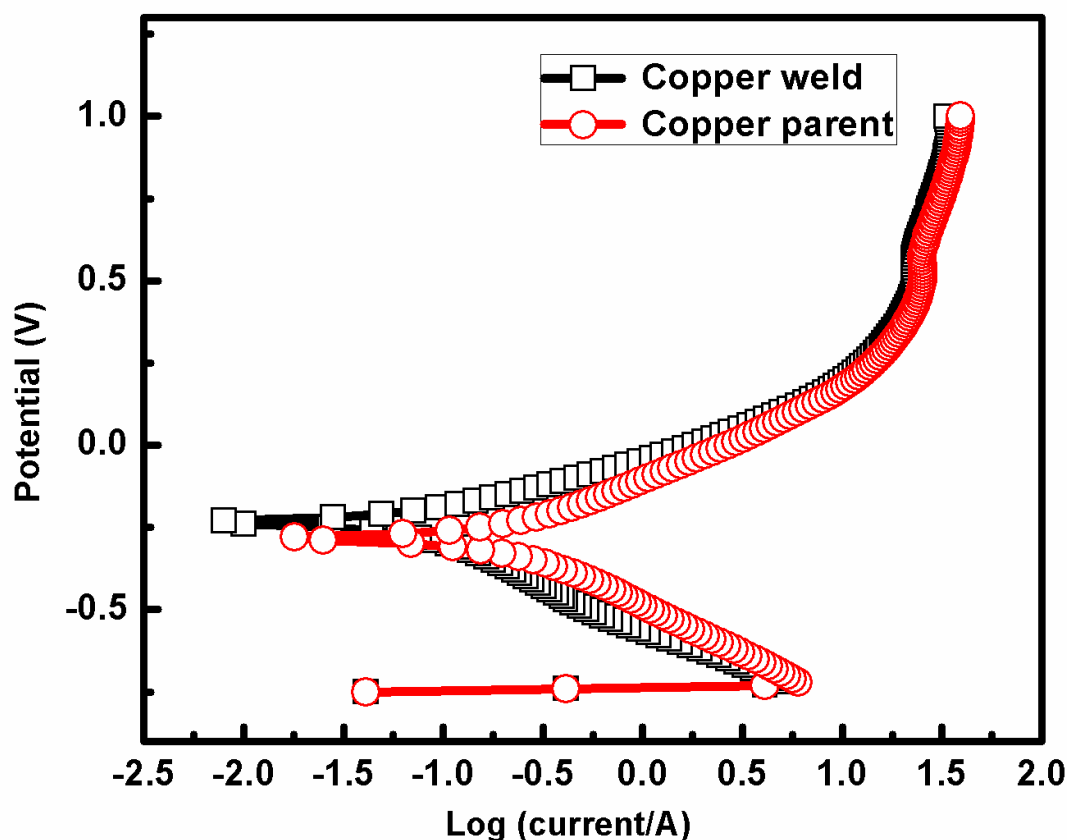


Figure 3. Potentiodynamic polarization curves of copper and friction stir welded copper-copper in 0.2N HCl



The results of the polarization curve are shown in Table 7 in presence of 0.2N HCl at room temperature. It is observed that the parent copper metal shows high corrosion rate of 0.01183 mm per year while friction stir welded copper imparts 0.0001228 mm per year and it has better corrosion resistance. It is also to be noted that the corrosion current is also higher for the parent metal compared to the welded junction. This result indicate that in the friction stir welded copper sample, the weld joint act as a cathode and give better resistance to corrosion when compared to parent copper plate.

Table 7:- Results of the polarization curve of parent copper and friction stir welded copper-copper plate

Sample	$i_{corr}$ (Corrosion current in mA/cm <sup>2</sup> )	Corrosion rate in mm/year	Corrosion rate in mpy	area of the plate in cm <sup>2</sup>	Polarisation Resistance $R_p$
Copper plate	3.615 E-6	0.01183	0.46	1	8477
FSW copper-copper	3.754E-8	0.0001228	0.0048	1	8.331E5

## Salt Spray and Immersion Methods

The results of salt spray method shown in Table 8 and immersion method in Table 9 are completely in agreement with the polarization data showing that the friction stir welded copper plate shows low corrosion rate compared to parent copper plate.

Table 8:- Salt Spray method

Sample	Medium	$\Delta W$ (mg)	CR=534 $\Delta W$ /DAT
Copper plate	5% NaCl	87	295.53mpy
Friction stir welded Copper-Copper	5% NaCl	93	176.02mpy

Table 9:- Immersion Method

Sample	Medium	$\Delta W$ (mg)	CR=534 $\Delta W$ /DAT
Copper plate	0.2 N HCL	570.0	216.19 mpy
Friction stir welded Copper-Copper	0.2 N HCL	587.8	92.81 mpy

In both the cases the weld metal (core zone) region, the metal behaves more corrosion resistance compared to parent material.

## Microstructure Analysis

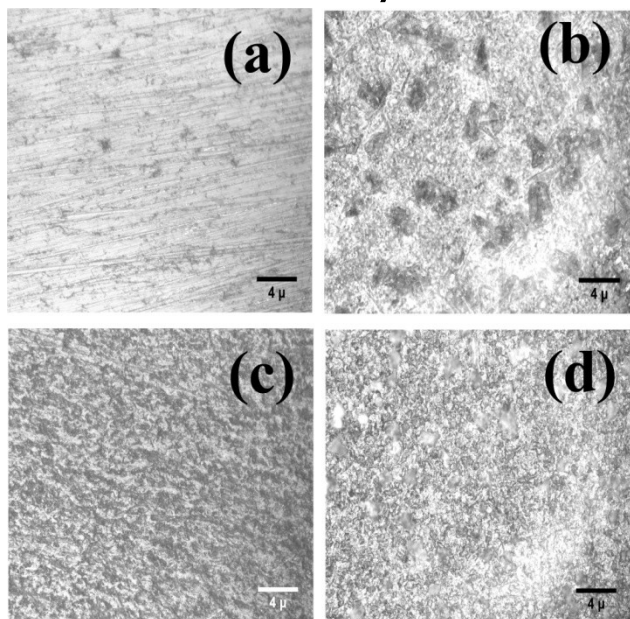


Figure 4. Microstructure of (a) brass parent (b) brass parent corroded (c) brass–brass weld and (d) brass–brass weld corroded plates.

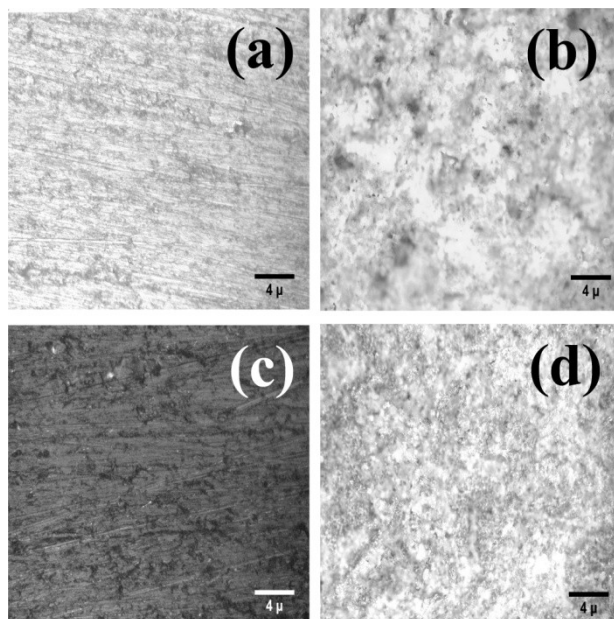


Figure 5. Microstructure of (a) copper parent (b) copper parent corroded (c) copper–copper weld and (d) copper–copper weld corroded plates.

The microstructural characterizations of the 950 rpm FSW conditions of both brass–brass and copper–copper plates were presented in Figure 4 (c) & Figure 5 (c) respectively. One can clearly observe joint has no defects or any other imperfections (lack of penetration, porosity etc..).

Comparison of Figure 4 (a) & 4 (c) (brass before FSW & after FSW) and Figure 5 (a) & 5 (c) (Copper before FSW & after FSW) clearly indicates the sample after FSW shows uniform grain size distribution.

After the corrosion studies were conducted for brass plates, Figure 4 (b) (parent brass after corrosion) shows high dominating pits indicating high corrosion damage whereas FSW brass–brass sample (Figure 4 (d)) shows comparatively very less number of pits after corrosion indicating a low corrosion rate.

Copper plates on observed after the corrosion studies shows, Figure 5 (b) (parent copper after corrosion) shows large number of pits indicating high corrosion damage whereas FSW copper–copper sample (Figure 5 (d)) shows comparatively very less number of pits after corrosion indicating a low corrosion rate.

## Hardness

Vickers Hardness values of parent and welded plates were shown in table 10 and it is observed hardness increased in welded plates as compared with parent plates. The reason may be attributed as large deformation twins and slightly elongated grain structures in parent plates. However, the elongated grain structure disappeared near the weld zone. The grain size was slightly increased by the annealing effect of welding heat. The exact central region of weld zone would have very fine and equiaxed grain structure due to the recrystallization caused by simultaneously received the plastic shear deformation and frictional heat.

Table 10:- Hardness studies

Sample	Copper plate	Copper weld	Brass plate	Brass weld
Hardness (HRB)	73.75	76	30	53.5

## Conclusion

The brass-brass and copper-copper plates were successfully welded using friction stir welding without failures or imperfections in the joints. On comparison with parent plates the Vickers hardness values showed an increment. Corrosion studies shows that the FSW plates are less prone to corrosion than parent plates. Moreover it is also observed from corrosion studies that the brass plates are more corroded when compared with copper plates and the reason for this can be attributed as dealloying in brass.

## References

- [1] 'Improvements relating to friction welding', W. M. Thomas, E. D. Nicholas, J. C. Needham, M. G. Murch, S. P. Temple, C. J. Dawes, *G. B. Patent No.9125978*, **8**, 1991.
- [2] 'Friction stir welding for the transportation industries', W. M. Thomas, E. D. Nicholas, *Materials and Design*, **18**, (4-6), pp.269-73, 1997.
- [3] 'Effects of friction stir welding on microstructure of 7075 aluminum', C. G. Rhodes, M. W. Mahoney, W. H. Bingel, R. A. Spurling, C. C. Bampton, *Scripta Materialia*, **36**, 1, pp.69-75, 1997.
- [4] 'Recent advances in friction-stir welding – Process, weldment structure and properties', R. Nandan, T. DebRoy, H. K. D. H. Bhadeshia, *Progress in Materials Science*, **53**, pp.980-1023, 2008.

- [5] 'Effect of tool position on the fatigue properties of dissimilar 2024–7075 sheets joined by friction stir welding', P. Cavaliere, F. Panella, *Journal of Materials Processing Technology*, **206**, pp.249–255, 2008.
- [6] 'On microstructural phenomena occurring in friction stir welding of aluminium alloys', A. Barcellona, G. Buffa, L. Fratini, D. Palmeri, *Journal of Materials Processing Technology*, **177**, pp.340–343, 2006.
- [7] 'Corrosion behavior of Al6061 alloy weldment produced by friction stir welding process', F. Gharavi, K. A. Matori, R. Yunus, N. K. Othman, F. Fadaeifard, *Journal of Materials Research and Technology* (IN press)
- [8] 'Recent Developments in Friction Stir Welding of Al-alloys', G. Cam and S. Mistikoglu, *Journal of Materials Engineering Performance*, **23**, 6, pp.1936–1953, 2014.
- [9] 'Enhancing mechanical properties of friction stir welded 2219Al–T6 joints at high welding speed through water cooling and post-welding artificial ageing', Z. Zhang, B. L. Xiao, Z. Y. Ma, *Materials Characterization*, **106**, pp.255–265, 2015.
- [10] 'Friction–stir welding of magnesium alloy AZ31B', J. A. Esparza, W. C. Davis, E. A. Trillo, L. E. Murr, *Journal of Materials Science Letters*, **21**, pp.917–920, 2002.
- [11] 'Friction stir processing of commercial AZ31 magnesium alloy', B. M. Darras, M. K. Khraisheh, F. K. Abu–Farha, M. A. Omar, *Journal of Materials Processing Technology*, **191**, pp.77–81, 2007.
- [12] 'Friction Stir Welding Studies on Mild Steel', T. J. Lienert, W. L. Stellwag, B. B. Grimmer, R. W. Warke, *Welding Journal, Research Supplement*, **82/1**, pp.1–9, 2003.
- [13] 'Structure, properties, and residual stress of 304L stainless steel friction stir welds', A. P. Reynolds, W. Tang, T. Gnaupel–Herold, H. Prask, *Scripta Materialia*, **48**, pp.1289–1294, 2003.
- [14] 'The joint properties of copper by friction stir welding', W. B. Lee, S. B. Jung, *Materials Letters*, **58**, pp.1041–1046, 2004.
- [15] 'Development of a fine-grained microstructure and the properties of a nugget zone in friction stir welded pure copper', G. M. Xie, Z. Y. Maa, L. Geng, *Scripta Materialia*, **57**, pp.73–76, 2007.
- [16] 'Microstructure and mechanical properties of friction stir welded copper', T. Sakthivel, J. Mukhopadhyay, *Journal of Materials Science*, **42**, pp.8126–8129, 2007.
- [17] 'Microstructures and mechanical properties of friction stir welds of 60%Cu–40% Zn copper alloy', H. S. Park, T. Kimura, T. Murakami, Y. Naganod, K. Nakata, M. Ushio, *Materials Science and Engineering A*, **371**, pp.160–169, 2004.
- [18] 'The joint properties of brass plates by friction stir welding', C. Meran, *Materials and Design*, **27**, pp.719–726, 2006.



- [19] 'Microstructural and mechanical properties of friction stir welded Cu-30Zn brass alloy at various feed speeds: Influence of stir bands', M. S. Moghaddam, R. Parvizi, M. H. Sabzevar, A. Davoodi, *Materials and Design*, **32**, pp. 2749–2755, 2011.
- [20] 'The effect of weld parameters on friction stir welding of brass plates', G. Cam, H. T. Serindag, A. C. akan, S. Mistikoglu, H. Yavuz, *Mat.-wiss. u. Werkstofftech.*, **39**, 6, pp. 394–399, 2008.
- [21] 'Electrochemical behavior of brass in 0.1 M NaCl', M. Kabasakaloglu, T. Kryak, O. Sendil, A. Asan, *Applied Surface Science*, **193**, 1–4, pp.167–174, 2002.
- [22] 'A comparative study on the passivation and localized corrosion of  $\alpha$ ,  $\beta$  and  $\alpha+\beta$  brass in borate buffer solutions containing sodium chloride-I. Electrochemical data' J. Morales, G. T. Fernandez, P. Esparza, S. Gonzalez, R. C. Salvarezza, A. J. Arvia, *Corrosion Science*, **37**, 2, pp.211–225, 1995.
- [23] 'A comparative study of the passivation and localized corrosion of  $\alpha$ -brass and  $\beta$ -brass in borate buffer solutions containing sodium chloride: III. the effect of temperature' J. Morales, G. T. Fernandez, S. Gonzalez, P. Esparza, R. C. Salvarezza, A. J. Arvia, *Corrosion Science*, **40**, 2–3, pp.177–190, 1998.
- [24] 'The effect of Cu-rich sub-layer on the increased corrosion resistance of Cu-xZn alloys in chloride containing borate buffer' I. Milosev, K. T. Mikic, M. Gaberscek, *Electrochimica Acta*, **52**, 2, pp.415–426, 2006.
- [25] 'A comparative study on the passivation and localized corrosion of  $\alpha$  and  $\beta$  brass in borate buffer solutions containing sodium chloride-III. X-ray photoelectron and auger electron spectroscopy data' J. Morales, P. Esparza, G.T. Fernandez, S. Gonzalez, J. E. Gracia, J. Caceres, R. C. Salvarezza, A. J. Arvia, *Corrosion Science*, **37**, 2, pp.231–239, 1995.
- [26] 'Electrochemical evaluation of the corrosion protection of bi-dimensional organic films self-assembled onto brass' F. Sinapi, S. Deroubaix, C. Pirlot, J. Delhalle, Z. Mekhalif, *Electrochimica Acta*, **49**, 17–18 pp.2987–2996, 2004.
- [27] 'Ethoxylated fatty acids as inhibitors for the corrosion of zinc in acid media' E. E. Foad El-Sherbini., S. M. Abdel Wahaab., M. Deyab. *Materials Chemistry and Physics*, **89**, 2–3, pp. 183–191, 2005.
- [28] 'Dissolution and Corrosion Inhibition of Copper, Zinc, and Their Alloys' P. Jinturkar, Y. C. Guan, K. N. Han, *Corrosion*, **54**, 2, pp.106–114, 1984.
- [29] 'Statistical Analysis of Electrode Kinetics Measurements-Copper Deposition from CuSO<sub>4</sub>-H<sub>2</sub>SO<sub>4</sub> Solutions' R. Caban, T. W. Chapman, *Journal of Electrochemical Society*, **124**, 9, pp.1371–1379, 1977.
- [30] 'Basic concepts of corrosion' L. L. Shreir, R. A. Jarman, G. T. Burstein, *Corrosion*, Vol 1, Metal/Environment

- [31] 'Impedance spectroscopic study of corrosion inhibition of copper by surfactants in the acidic solutions' H. Ma, Sh. Chen, B. Yin, Sh. Zhao, X. Liu, *Journal of Corrosion Science*, **45**, 5, pp.867–882, 2003.
- [32] 'Electrochemical behaviour of copper electrode in concentrated sulfuric acid solutions' A. H. Moreira, A. V. Benedetti, P. L. Calot, P. T. A. Sumodja, *Electrochimica Acta*, **38**, 7, pp.981–987, 1993.